Thermal Assessment of Glass Façade Panels under Radiant Heating: Experimental and Preliminary Numerical Studies

Chiara Bedon[1*], Marcin Kozłowski[2,3], Dániel Honfi[4]

* Corresponding author
1 University of Trieste, Italy, chiara.bedon@dia.units.it
2 Lund University, Sweden
3 Silesian University of Technology, Poland
4 RISE - Research Institutes of Sweden, Sweden

Abstract

Nowadays, glass is increasingly being used as a load-bearing material for structural components in buildings and façades. Different structural member solutions (such as panels, beams, columns) and loading conditions were the subjects of several research studies in recent years. Most of them, however, were typically limited to experimental testing and numerical simulations on glass elements and assemblies at room temperature. Thermo-mechanical investigations, inclusive of the temperature-dependent behaviour of visco-elastic interlayers used in laminated glass solutions, as well as the typical thermo-mechanical degradation of glass properties in line with temperature increase, in this regard, are still limited. Such an aspect can be particularly important for adaptive façades, in which the continuous variation of thermal and mechanical boundary conditions should be properly taken into account at all the design stages, as well as during the lifetime of a constructed facility. Given the key role that thermo-mechanical studies of glazing systems can pe use of glass in façades, this paper focuses on Finite Element (FE) numerical modelling of monolithic and laminated glass panels exposed to radiant heating, by taking advantage of past experimental investigations. In the study discussed herein, being representative of some major outcomes of a more extended research project, one-dimensional (1D) FE models are used to reproduce the thermal behaviour of selected glass specimens under radiant heating, as observed in the past experiments. Given the high computational efficiency but very basic assumptions of 1D assemblies, a critical discussion of experimental-to-numerical comparisons is then proposed for a selection of specimens.

1   INTRODUCTION

Façade systems, both traditional and innovative (i.e. adaptive façades that have been gaining widespread attention recently), are subjected to a multitude of boundary and loading conditions over their lifetime, including thermal and mechanical variations. In this regard, the system behaviour, especially for adaptive façades, should be properly assessed by giving careful consideration to several loading combinations, since these are responsible for degradation phenomena at material, component, and assembly level (Bedon, 2017; Bedon et al., 2018c). This is especially true when considering structural issues for façades in general, where both full-scale experiments and Finite Element (FE) numerical models that are able to capture the actual material and assembly behaviours are often required.

In this paper, the thermo-mechanical performance of glass façade panels is the subject of preliminary investigation, via experimental testing and simplified FE numerical methods. Glass, as commonly known, is largely used in engineering applications as a structural material, especially in the form of laminated sections composed of multiple glazing layers, bonded together by thermoplastic foils (see for example (Haldimann, Luible, & Overend, 2008; Feldmann et al., 2014)). However, major issues in the design of structural glazing assemblies are represented by the high sensitivity of glass and common bonding layers to temperature variations.

In recent years, several research studies have focused on the thermal and optical assessment, or energy performance evaluation, of several types of glazing assemblies and solutions, both at the component and at the whole building level (see for example Fang, Eames, & Norton, (2007); Ghosh, Norton, & Duffy (2016); Ghoshal & Neogi, (2014); Li, Li, Zheng, Liu, & Lu (2015); Aguilar et al. (2017); Parra, Guardo, Egusquiza, & Alavedra (2017), etc.).

From a structural point of view, the thermal performance of glass elements and systems directly reflects upon their load-bearing capacity, due to the intrinsic material properties (see Bedon (2017), for example, for a state-of-the-art review on load-bearing structural glass systems under fire). The key role of appropriate thermo-mechanical investigations is further enforced in the case of adaptive façades, rather than in traditional static curtains, where glass components could be further affected by continuous variations in both the thermal and mechanical boundary conditions (Favoino, Jin, & Overend, 2014; Hasselaar & Looman, 2007; Aldawoud, 2017; Baumgärtner, Krasovsky, Stopper, & von Grabe, 2017; etc.). On one side, given a daily or accidental/extreme temperature variation, thermal shock phenomena occurring after moderate/high thermal gradients can cause changes that exceed the strength of the glass, leading to opening and propagation of cracks, with loss of the structural integrity (Cuzzillo & Pagni, 1998; Tofilo & Delichatsios, 2010; etc.). Glass systems, due to the typically low material resistance and low thermal conductivity (Haldimann et al., 2008), are particularly vulnerable to failure from thermal shock (see for example Fig. 1(a)).

At the same time, the degradation of mechanical properties of the glass brought about by high temperature (modulus of elasticity, tensile resistance, etc.) could severely affect the structural performance of such assemblies (see Fig. 1(b)). On the other hand, the well-known temperature/load-time dependent behaviour of viscoelastic interlayer and/or rubbery materials that are commonly used to bond together the glass panels, as well as to join the glass panels to the structural background (see (Haldimann et al., 2008)) can have crucial effects even under operational conditions. At the design stage, the combination of these multiple phenomena should be hence properly accounted for, for safe design purposes.
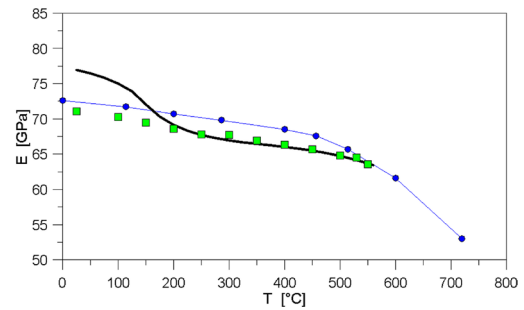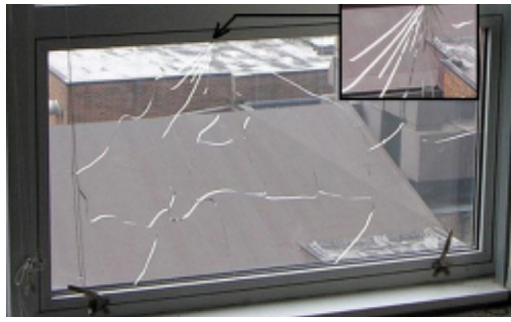
FIG. 1 Glass systems under thermal loading: (left) examples of thermal shock phenomena in a glass window and (right) experimental variation with temperature of the modulus of elasticity of ordinary glass *(figure adapted with permission from Bedon (2017) - plots are derived from different investigations)*

Experimental research studies have been focused, in the last few years, on the assessment of the thermo-mechanical performances of glass windows, façade systems, small-scale components subjected to high temperature scenarios and/or fire loading. Thermo-mechanical investigations on glazing systems, however, are indeed still limited in number and structural typology. An increasing interest is captured especially by the performance of structural glass components under fire, due to safety purposes. While full-scale experimental studies are still rare in the literature (see Bedon (2017) for an overview), numerical modelling can represent a robust tool and support for designers, as a further extension of time consuming and expensive testing. Key input parameters and possible limits in the same FE method, however, should be properly taken into account.

Bedon, Pascual Agullo, Luna-Navarro, Overend, & Favoino (2018b) numerically investigated the thermal and structural performance of glass-to-GFRP sandwich façade modular units, under ordinary thermal conditions and wind pressure. Although limited to specific loading configurations, the study suggested the importance of coupled thermal and mechanical simulations for a given glazing system, which should be preferably taken into account to optimise its overall performance. Bedon & Louter (2018) numerically investigated the load-bearing response of laminated glass plates under standard fire ISO curve and imposed mechanical loads. The numerical analyses generally gave evidence of a close correlation with test results, even suggesting the extension of the same study to a wide set of thermal-to-mechanical loading ratio conditions. At the same time, the mechanical restraints were found to have a crucial role in the overall performance of the same glass plates, both from the thermal and numerical points of view.

In this paper, numerical simulations are carried out in ABAQUS (Simulia) and proposed for both monolithic and laminated glass specimens under radiant heating, by means of geometrically simplified but computationally efficient one-dimensional (1D) assemblies. In doing so, the major advantage is taken from available experimental results, for small-scale glazing samples under thermal loading. Comparative results are then critically discussed, based on selected experimental results, in order to emphasise the potential and possible criticalities of the FE method. The research outcomes partly summarised in the paper are derived from two Short-Term Scientific Missions (STSMs) by the involved authors (WG2 - "Structural" Task Group members), which has been approved and financially supported, throughout 2018, by the EU-COST Action TU1403.

2 SUMMARY OF THE REFERENCE EXPERIMENTAL CAMPAIGN

The numerical analyses presented in this paper are based on the results of past experimental studies. Debuyser et al. (2017) carried out an experimental campaign that aimed to assess the thermal behaviour of annealed monolithic or laminated glass samples (annealed glass plies bonded together with PVB and SGP interlayers). In the reference study, glass panels with nominal dimensions of 185mm × 285mm were mounted in a supporting frame and exposed to radiant heating. See Fig. 2.

FIG. 2 Radiant panel tests *(debuyser, 2015; Debuyser et al., 2017)* (left); heat flux meters mounted on the frame, (right) testing of a sample

SAMPLE #	GLASS THICKNESS / BUILD-UP [MM]	INTERLAYER THICKNESS
T2	10 (MG)	-
T4	15 (MG)	-
T5	6+10+6 (LG)	0.76 mm (PVB)
T12	6+10+6 (LG)	0.76 mm (PVB)

TABLE 1 Overview of selected test specimens, according to *(Debuyser, 2015; Debuyser et al., 2017)*
Key: MG= monolithic glass, LG= laminated glass

The distance between the radiant panel and the typical glass specimen was about 450mm. All of the experiments started at an imposed air flow and gas flow of 8l/s and 0.475l/s, respectively. However, a time dependent decrease of the same gas flow (and hence of the corresponding heat flux) was generally observed during the tests. See Fig. 3.

Besides measuring the surface glass temperature (based on a set of thermocouples mounted both on the exposed and unexposed sides of each sample), the heat flux was also continuously monitored throughout the tests. This was done by means of Gardon gauge type sensors, which use a differential thermocouple as a transducer to measure the temperature difference between the centre and the circumference of a thin circular foil disc. The latter is bonded to a circular opening in a cylindrical heat sink. See Fig. 2(left).

Moreover, within the same experimental study, additional test measurements of thermal properties such as conductivity, diffusivity, and volumetric heat capacity of glass and PVB/SG interlayers were carried out. Further details of the tests results can be found in Debuyser (2015).
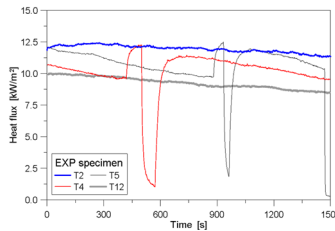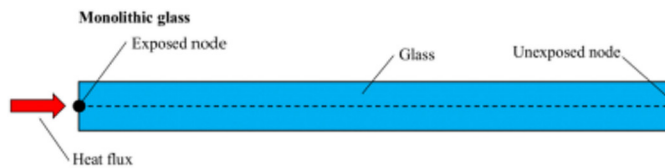
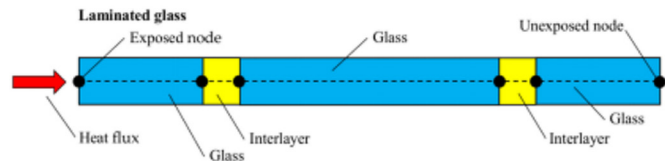FIG. 3 Measured heat flux (at the side of the samples) for the selected tests specimens T2, T4, T5, and T12

FIG. 4 Schematic representation of 1D heat transfer models (ABAQUS). Typical view of (above) monolithic and (below) laminated glass specimens

From the total number of 16 specimens discussed in Debuyser, (2015) and Debuyser et al., (2017), four sets of glass samples were selected for the current study. In Table 1, the samples labelled as T2 and T4 represent monolithic glass panels with a thickness 10mm and 15mm, respectively. Specimens T5 and T12 are both laminated glass samples, composed of two external, 6mm thick glass plies each side of a central 10mm ply (0.76mm is the nominal thickness of the bonding PVB foils).

Fig. 3 presents the measured heat flux at the side. From the figure, slightly declining values of the heat flux for all specimen can be observed. The phenomenon is strictly related to the specifics of the radiant panel, in which constant heat flux was very difficult to obtain. Moreover, for the specimens T4 and T5 sudden drops of the heat flux at approx. 500s and 900s can be seen. These drops were caused by the unintentional overheating of the radiant panel, which was followed by the shutting off of the device. However, in these cases, the radiant panel was powered on again and the tests were continued.

3   NUMERICAL SIMULATIONS

The main aim of the numerical study summarised herein was to simulate the thermal behaviour of monolithic and laminated glass panels subjected to the assigned heat flux histories. In doing so, a one-dimensional (1D) heat transfer modelling approach was initially chosen, due to the well-known computational efficiency, in order to assess the potential and possible limits, compared to more advanced and refined (but time-consuming) full solid 3D models. The numerical results and comparisons discussed herein, in this regard, represent some major outcomes of an extended investigation. In the FE study, the set of samples summarised in Table 1 was numerically analysed by taking into account the experimental heat flux measured during the tests.

In accordance with the adopted 1D modelling approach, given a glass sample under thermal loading, the absorbed energy is conducted through the monolithic glass or through the different layers of

the glass laminates, thereby causing a temperature increase within the materials. To describe this absorption and conduction, several temperature dependent thermal properties of both the glass and the interlayers are required, namely the specific heat capacity, the density, and the thermal conductivity. The temperature increase within the specimen is then estimated as the net result of the absorbed heat flux and the cooling heat fluxes. Therefore, the radiative and convective heat transfer to the environment are modelled at both the exposed surface and the back surface. The radiation to the environment requires the surface emissivity as input, and is assumed to be lumped at the surfaces of interest. The convection is then calculated as a function of the convective heat transfer coefficient. As the convective heat transfer coefficient is dependent on the nodal temperatures calculated within the given FE model, a user subroutine is required to describe its evolution (see Section 3.1). The basic assumption of such a FE modelling strategy is that three-dimensional effects (i.e. in-plane heat flux variations or in-plane temperature gradients, in combination with the imposed through-the-thickness heat flux) can be disregarded. The experimental-to-numerical comparisons are therefore reliable as long as the test temperatures from the past samples are measured in the central part of the glass panels, where the in-plane temperature gradient is negligible (see Section 2).

Careful consideration was given to the post-processing, especially for the FE analysis of the amount and evolution of temperature on the specimens' surfaces (both exposed and unexposed to the imposed heat flux), as well as the influence of heat flux history on the glass thermal response, including the temperature gradient DT in the thickness of each sample, throughout the simulation time. The latter aspect (manually calculated as the difference of temperature at the exposed and unexposed nodes) is a particularly important parameter because it is directly related to potential failure of glass due to thermal shock phenomena.

3.1   MODEL DESCRIPTION

A one-dimensional (1D) heat transfer model, analogous to the modelling approach presented in Debuyser (2015) and Debuyser et al. (2017), and further developed in Bedon, Honfi, & Kozłowski (2018a), was created using the commercial computer software ABAQUS (Simulia). The typical 1D model consisted of 2-node, one-dimensional diffusive heat transfer elements (type DC1D2, from ABAQUS element library), (Fig. 4). Temperature dependent thermal properties of glass and interlayers, such as conductivity and specific heat, were taken from references in literature (Tong, 1994; Cardenas, Leon, Pye, & Garcia, 2016; Debuyser, 2015). An optimal emissivity coefficient equal to 0.97 was then assumed for the glass surfaces, based on previous sensitivity studies (Bedon et al., 2018a). To define the thermal boundary conditions between the external glass nodes and the surrounding environment, a Fortran script user-subroutine was used. This involved a convective heat transfer coefficient dependent on the varying temperature of the exposed and unexposed nodes, as also described in detail in Debuyser (2015), Debuyser et al. (2017), and Bedon et al. (2018a). In doing so, long-wave radiative phenomena and related effects were neglected. While long-wave exchanges typically have a key role in energy balance simulations in buildings and require advanced numerical tools (see for example Stefanizzi, Wilson, & Pinney (1990) Miller, Thomas, Kämpf, & Schlueter (2015) etc.), they are mostly negligible and conventionally disregarded for thermo-mechanical engineering simulations on ordinary, soda lime silica glass systems (Tong, Zhu, Guo, & Ma, 2002; Wang, Wang, & Li, 2013; Wang & Wang, 2016; etc.). An initial ambient temperature of 20°C was applied to the typical FE model. In the simulations, additional physical constants were also taken into account, such as the Stefan-Boltzmann constant (5.67×10^{-8} W/m^{2}K^{-4}) and the absolute zero temperature (–273°C). The thermal exposure was finally simulated by applying a concentrated heat

flux to the exposed node of each 1D model, by taking into account - for each sample - the heat flux histories from the experiments.

Sections 3.2 and 3.3 present some selected results for the monolithic and laminated glass samples object of investigation. There, continuous lines are conventionally used to represent the temperature evolution at the exposed node of each specimen ("Exp", in the following), while dashed lines are used for the unexposed node ("UnExp").

3.2   NUMERICAL RESULTS FOR MONOLITHIC GLASS SPECIMENS

Fig. 5 presents a comparison of numerical and experimental results for the 10mm thick monolithic glass specimen (T2, according to Table 1). In the past experiment, the specimen T2 was exposed to a constant heat flux slightly decreasing over time, (Fig. 3). Such a thermal loading typically resulted in a rather stable increase of temperature over time in the thickness of the sample(Fig. 5(a)). In general, the FE model proved to offer a rather acceptable agreement with the corresponding test measurements. However, the numerical results were found to partly overestimate the experimental predictions. A close correlation was observed especially at the beginning of the temperature history (≈300s), at both the exposed/unexposed nodes. For the following instances of thermal exposure, the average scatter was found to grow to a maximum of 12%, which may be related to the input parameters assumed herein, and in particular the thermo-physical properties of glass.

Fig. 5(b), in this regard, shows a point-by-point comparison between the experimentally and numerically estimated temperatures, on both the exposed and unexposed faces of the T2 specimen. Input data are taken from selected time instants (0-1500s) and proposed in normalised form. Given the linear trend of both the series of dots, it is possible to notice that through the full thermal exposure the numerical data estimate the experiments in the average value of 10% and 5%, at the exposed and unexposed nodes, respectively. The experimental-to-numerical correlation, in addition, has mostly a linear trend for both the reference control points, with major scatter in the range of 130-180°C only (approx. 300-500s).

Additional experimental-to-numerical results are finally proposed, for the same T2 sample, in Fig. 5(c), in the form of temperature gradient DT in the thickness of glass. As expected, the numerical results were observed to generally overestimate the experimental calculations, up to approx. 50% in some exposure intervals. Such a scatter, resulting from cumulative effects depicted in Fig. 5(b), was found to have a mostly uniform trend for the full time history. This effect could be caused by the input thermal parameters of glass, as previously highlighted, but also by possible defects of the measurement methods, as partly described by Bedon et al. (2018a). In terms of thermal cracking for the examined specimen, both the experimentally and numerically calculated temperature gradients DT are presented in Fig. 5(c) and lie below the allowable value of 45°C that the prEN thstr:2004 document recommends for annealed glass panels with polished edges (10mm the nominal thickness, as in the case of the T2 sample), to prevent thermal shock.
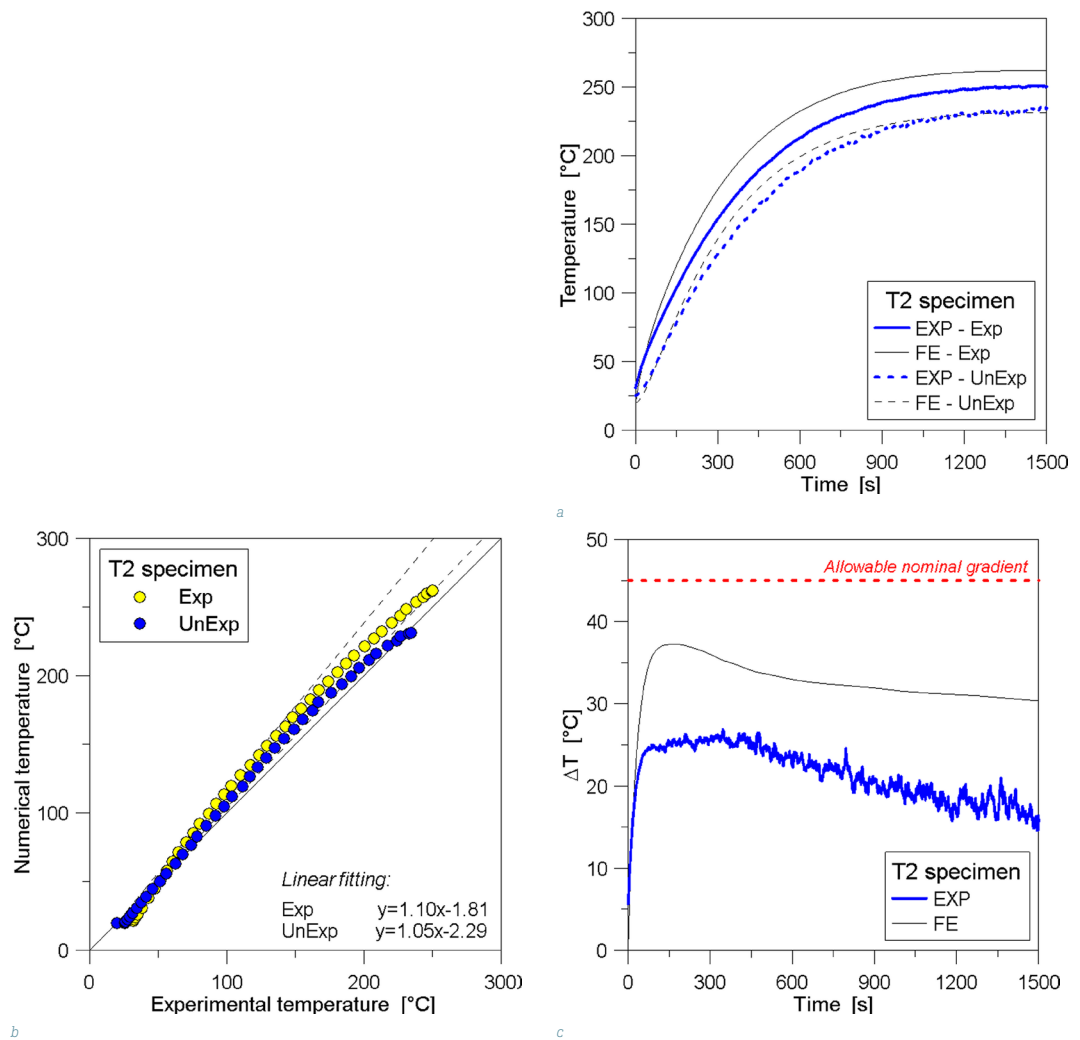
FIG. 5 Comparison between experimental and numerical (ABAQUS) results for the monolithic T2 sample: (a) temperature history and (b) point-by-point temperature comparisons for selected time instants, with (c) calculated temperature gradient, as a function of time

GLASS TYPE	LIMIT VALUES (°C)		
	As-cut or arrissed	Smooth ground	Polished
Float or sheets ≤12mm thick	35	40	45
Float 15mm or 19mm thick	30	35	40
Float 25mm thick	26	30	35
Patterned	26		
Wired patterned or polished wired glass	22		
Heat strengthened	100		
Tempered	200		
Laminated	Smallest value of the component panes		

TABLE 2 Allowable temperature gradients, according to prEN thstr:2004 provisions

For clarity of presentation, Table 2 reports the actual reference values for different glass types and treatments, according to the same prEN thstr:2004 provisions. No major cracks due to thermal

loading were observed during the experiment, even if limited damage propagation was noticed close to the sample supports, at the edge of the T2 panel, after 18min (≈1000s) of exposure). According to Fig. 5(c), such a time instant corresponds to a limited temperature gradient (≈22°C), hence suggesting further studies are necessary.

With the 15mm thick, monolithic specimen T4 being taken into account - with a difference from the T2 sample represented by the nominal thickness and the assigned radiant heating (Fig. 2, "T4 EXP" plot) - the temperature estimations proposed in Fig. 6 were obtained.
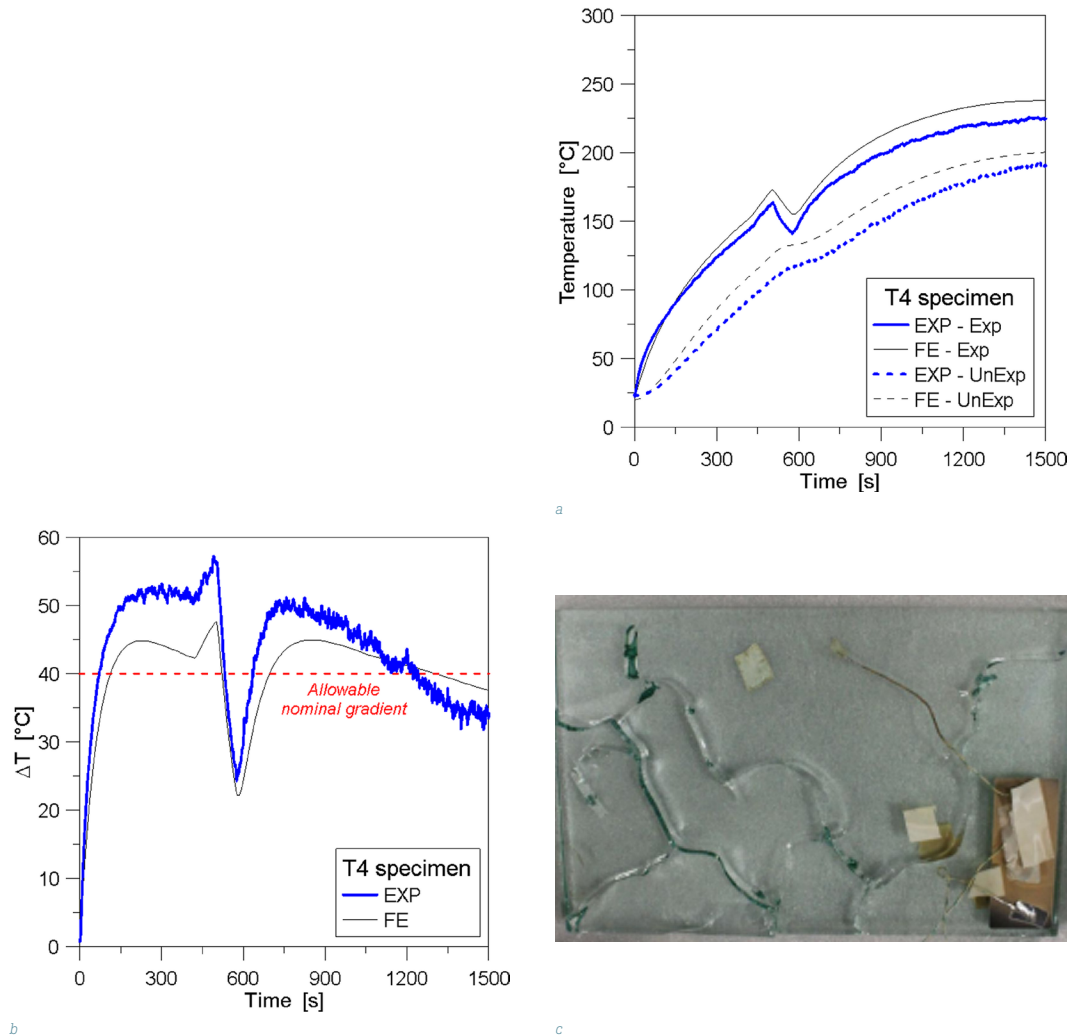
a

b

c

FIG. 6 Comparison between experimental and numerical (ABAQUS) results for the monolithic T4 sample: : (a) temperature history and (b) calculated temperature gradient, as a function of time, with (c) experimentally observed cracks in the sample

As in the case of the T2 specimen, the numerical results were generally observed to slightly overestimate the experimental data (Fig. 6(a)). For the FE node exposed to the heat flux, much better correlation was found, especially at the beginning of the temperature history (up to 600-700s), rather than at the later stage of the analysis (where, in any case, the FE temperature values exceed fewer than 10% the corresponding test results). In the case of the unexposed node, for the whole simulation

time, the FE results were indeed found to overestimate the experimentally measured temperatures, by approximately 10%. For both the exposed and unexposed nodes, after ≈500s of thermal exposure, a drop in temperature can be also clearly observed, which was caused by a sudden shutting off of the radiant panel. Such a phenomenon is more evident on the exposed surface, while the unexposed node - due to the thermal inertia of glass volume - is less sensitive.

Fig. 6(b) shows the temperature gradient ΔT as a function of time, as calculated from the past experimental data and obtained from the numerical analysis of the T4 specimen. As shown, the numerical results were observed to underestimate the experiments until approximately 1200s of exposure, while, subsequently, the FE predictions overestimate the experiments. The measured and simulated ΔT was much larger than the allowable temperature gradient recommended by the prEN thstr:2004 provisions (i.e. 40°C for 15mm thick polished panels, see Table 2) and was typically associated - in the reference experiments – with severe cracks in the specimen, (Fig. 6(c)). Since the numerical gradient of Fig. 6(b) also rises up to ≈22°C, given the mechanical properties of glass (i.e. Fig. 1(b), etc.) and its sensitivity to temperature variations, it is also expected that the thermo-mechanical analysis of the same sample - typically requiring a time-temperature scenario for the FE model nodes as a key input parameter - could also result in crack propagation.

3.3 NUMERICAL RESULTS FOR LAMINATED GLASS SPECIMENS

Two selected laminated glass specimens were then taken into account from the full set of experimental samples, with the reference cross-section schematised in Fig. 7.
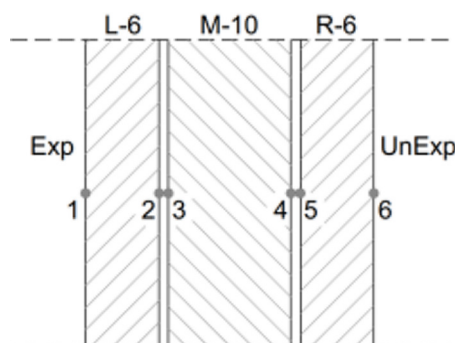

FIG. 7 Reference layered section for the laminated T5 and T12 specimens, with evidence of numerical control points

Fig. 8, in this regard, presents a comparison of numerical and experimental results for a laminated glass specimen composed of two 6mm plies and a middle 10mm ply (T5, see Table 1). Even moving from a monolithic to a layered cross-section, as also observed for the T2 and T4 results, much better agreement with the experiments was observed for the early stage of the FE analysis on the T5 assembly (600-700s). This included the evolution of temperature at both the exposed an unexposed nodes. During the reference experiment, similarly to the T4 sample, a sudden shutting off of the radiant panel took place at approx. 950s of exposure. Such an accident can be clearly perceived in the temperature histories shown in Fig. 8(a). Given the presence of multiple glass layers - compared to the T4 monolithic sample - it is, in any case, possible to notice that the temperature records were affected on the exposed surface only, with mostly null effects on the back face of the laminated assembly. Worth noting, finally, is that after 700-800s of exposure, the FE model generally proved

to underestimate the test results for the exposed node (up to -15% their scatter at the final stage of the analysis). Conversely, the temperature evolution was overestimated for the unexposed glass layer (up to +30%, at the end of the analysis). A similar result could be derived both from the input thermal properties of glass and interlayers, as well as from the basic assumptions of the 1D models presented herein, hence suggesting the need for further extended investigations.
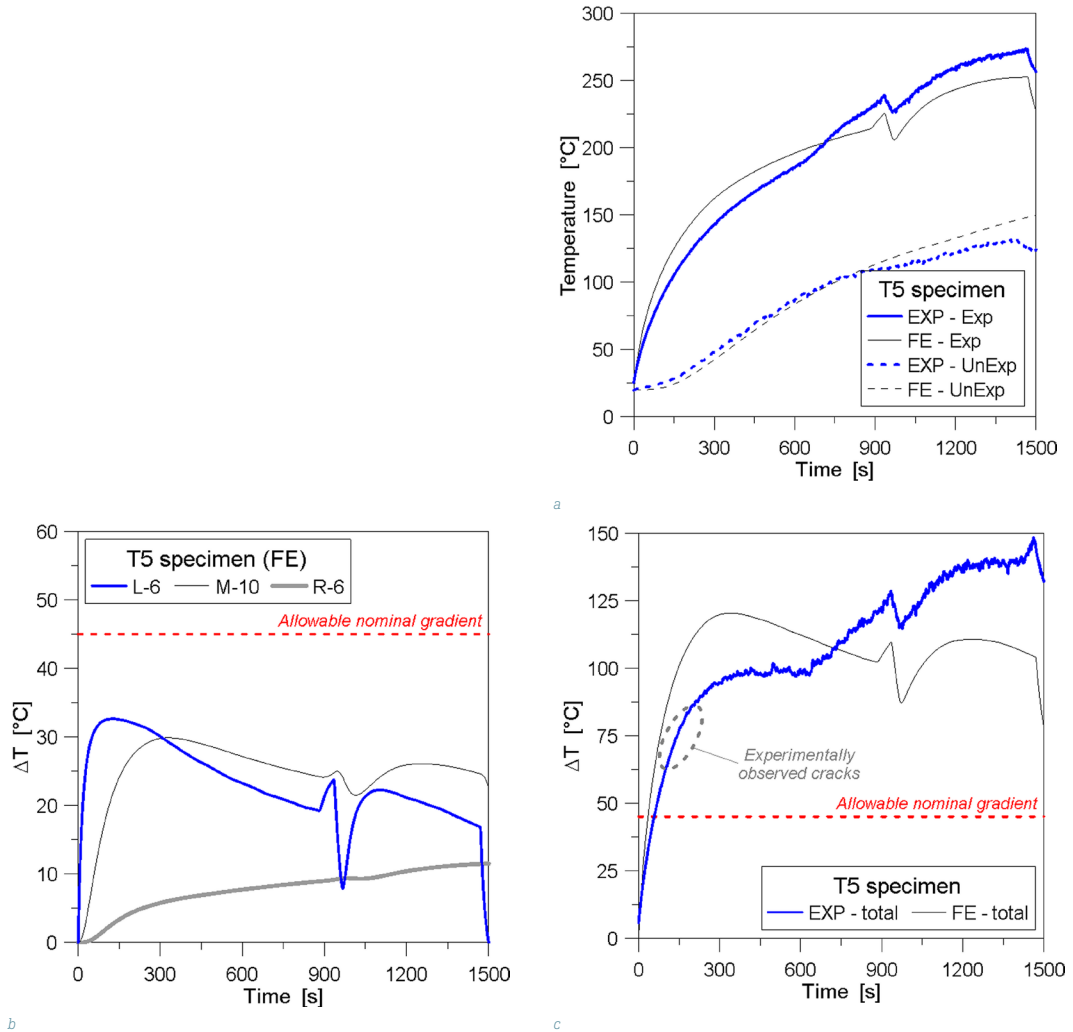

FIG. 8 Comparison between experimental and numerical (ABAQUS) results for the laminated T5 sample: (a) temperature history; (b) numerically calculated temperature gradient for all the laminate plies, as a function of time and; (c) absolute / total gradient for the T5 sample, as obtained from the test and the FE model

Additional comparative calculations were then carried out by taking into account the FE temperature gradient over time, through the thickness of the sample. Fig. 8(b) presents temperature gradients for each ply, as obtained from the T5 numerical simulation. At the time of the experimental investigation - for the laminated specimens - no additional thermocouples were mounted within the thickness of the given sandwich section, but only at the external faces of the samples. Consequently, no direct DT comparisons can be carried out for each glass ply, and the FE results in Fig. 8(b) can offer qualitative feedback only. As shown, the exposed surface ("L-6" plot) heats up the fastest, and an high temperature gradient (> 30°C) is predicted at an early stage of the simulations (≈130s).

The middle, 10mm thick glass ply ("M-10") shows a DT evolution in time of lower magnitude, due to the protective contribution of the exposed layer (≈ 30°C the maximum DT prediction), as well as a certain delay in the temperature increase (≈250s). The middle layer itself insulates the unexposed glass ply, which shows limited DT values (in the order of 50% the other plies, "R-6" plot) and a totally different evolution in time. In Fig. 8(b), the sudden drop of DT for the exposed L-6 ply can still be observed at approx. 950s of exposure, in accordance with the experimental findings. With regard to the examination of the middle and unexposed glass layers, mostly null effects can be perceived from the same heat flux drop.

For laminated glass systems (Table 2), the thermal fracture is conventionally ensured insofar as the allowable nominal gradient for the weakest ply is not exceeded, according to the existing recommendations. In the case of the T5 laminated assembly (as well as the T12 specimen discussed in the following chapters), the experimental crack was observed to initiate in the range of 230-260s of exposure. In this regard, the absolute/total gradient for the sample of investigation can offer some further feedback on its overall performance. In Fig. 8(c), the absolute variation is shown, over time, for the temperature measurements at the exposed and unexposed nodes (i.e. assuming a fully monolithic performance for the laminated cross-section). Compared to the reference nominal value of 45°C (Table 2), it can be observed that the experimental cracks were typically observed to propagate for absolute thermal gradients in the order of 60-70°C. The actual effect of the intermediate PVB foils for the nominal layered section (Fig. 7), however, requires further extended investigations.

In Fig. 9, finally, comparative results are shown for the T12 laminated specimen, having the same geometrical and mechanical properties of the T5 sample (Fig. 7). In accordance with earlier observations, a close agreement with the experiments was observed, especially for the early stage of the FE analysis (600-700s, with less than 10% of scatter). At approximately 600s of exposure, however, a marked increase of experimental temperatures for the exposed node can be observed. Such an effect can be justified, most probably, by the detachment of the aluminium foil shielding the thermocouple of interest from direct radiation. A mostly linear trend was, in fact, recorded for the heat flux (Fig. 3), thereby excluding possible abrupt variations in the loading condition. For the same reason, a mostly stable temperature increase was numerically predicted for the exposed node, hence resulting only in an apparent mismatch between the compared curves (15-20% their scatter at the final stage of the experiment). In the case of the unexposed node, similarly to the T5 specimen, the FE analysis generally overestimated the corresponding test data, with increasing scatter towards the final phase of thermal exposure (+30%, after 1500s of testing). The close correlation with T5 observations (Fig. 8(a)) can be considered as a suggestion for possible 1D modelling limitations, requiring the use of more refined FE models able to capture the actual performance of the laminated specimens.

With regard to the temperature gradient in each glass layer that were taken into account for the T12 assembly (Fig. 9(b)), a close qualitative correlation with the T5 numerical predictions can again be perceived. Some minor variations in Figs 8(b) and 9(b) are related to the different input thermal loading for the T5 and T12 samples (see Fig. 3). Accordingly, the exposed glass ply is subjected to > 25°C of thermal gradient in the first 150s of exposure. The middle glass layer suffers a lower and delayed DT increase (-15% the exposed ply, after 300s of thermal loading). The unexposed glass layer, finally, is mostly protected by the other assembly components. A maximum DT in the order of 10°C can be noticed only after 1500s of exposure.
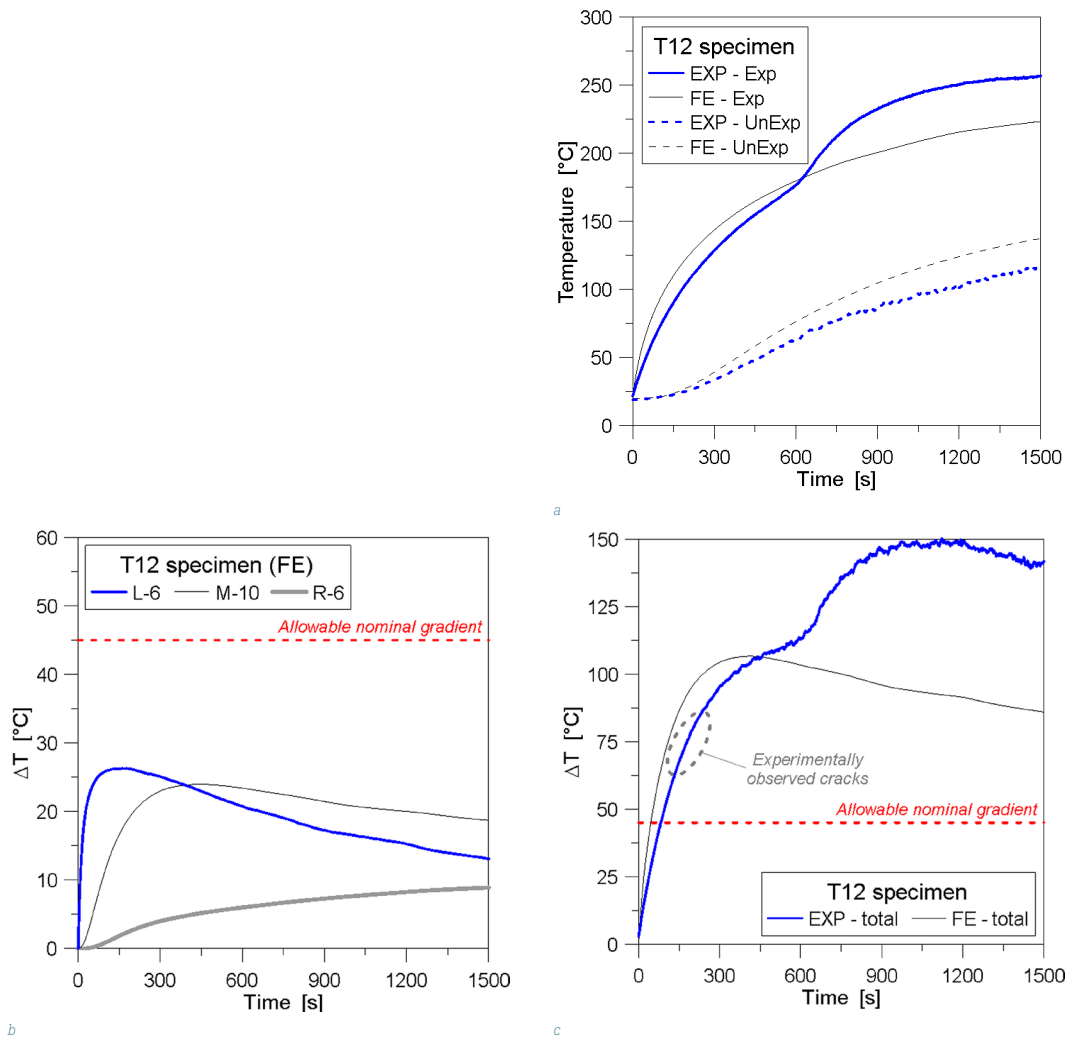
FIG. 9 Comparison between experimental and numerical (ABAQUS) results for the laminated T12 sample: (a) temperature history, (b) calculated temperature gradient for all the laminate plies, as a function of time and (c) absolute / total gradient for the T5 sample, as obtained from the test and the FE model

In Fig. 9(c), finally, a qualitative agreement can again be observed between the T12 and T5 fracture performance, insofar as the layered cross-section of Fig. 7 is roughly approximated to an equivalent, fully monolithic section. In this regard, further investigations are required to capture the contribution of common interlayer foils for the overall thermo-mechanical performance of glass laminates, both from a pure thermal point of view, as well as in terms of mechanical efficiency, given the limited resistance and shear stiffness of these films to high temperatures. The effect of simplified numerical approaches for laminated sections under radiant heating and fire, in particular, needs to be assessed in terms of experimental data.

4   SUMMARY AND CONCLUSIONS

In this paper, some selected results from a research collaboration between the involved authors were presented, as obtained during two Short-Term Scientific Missions (STSMs) approved and financially supported in Spring 2018 by the EU-COST Action TU1403 "Adaptive Façades Network", as well as from the excellent networking activity that still follows the same STSMs. During the joint research project, special care was given to the development of a reliable thermo-mechanical model for monolithic and laminated structural glazing at elevated temperatures. Further studies would require the calibration of several input features, especially those being the key influencing parameters of both thermal and mechanical aspects of relevance on the overall structural performance of these systems.

As a first step, one-dimensional (1D) models were used to study the thermal behaviour through the cross-section of glass plies. The typical heat transfer FE analysis was validated against previous experimental investigations, where glass specimens with several geometrical and mechanical features have been exposed to radiant heating, resulting - in some cases - in breakage of the panels. Although the adopted FE modelling approach includes several simplifications - first of all the lumped thermal performance of the glass plates object of analysis - interesting conclusions can be drawn and used in the future developments of more refined thermo-mechanical models.

One major challenge in the FE assessment of the structural performance of glass systems under thermal loading is that the available information on the temperature dependence of various thermo-physical and mechanical material properties in the literature is scarce. Therefore, experimental testing is generally highly valuable. However, testing glass samples and assemblies at high temperatures is commonly challenging, time-consuming and costly. Furthermore, the measurements themselves can include difficulties and uncertainties (see for example Bedon et al. (2018a)). It requires careful planning to decide how the temperatures and heat fluxes are measured to obtain the relevant information for the validation of the numerical models.

In terms of numerical modelling, 1D assemblies are typically associated with a well-known computational efficiency, but also to marked simplifications in their input features and expected results. In this regard, compared to more detailed two-dimensional (2D) or three-dimensional (3D) numerical models, 1D systems are not able to account for several key aspects for thermo-mechanical simulations, such as:

— Thermal boundary effects (i.e. thermal exposure of the samples faces to the assigned thermal load)
— Mechanical boundary effects, namely represented by the temperature distribution and evolution in time, in the contact regions between the glass specimens and the supports (and/ or the test setup components, etc., typically consisting of different materials with specific thermo-mechanical features)
— Size effects, being the 1D (and 2D) models intended to predict the temperature distribution in a given ideal section of the specimen under investigation, i.e. disregarding edge effects and other local phenomena

The sensitivity of similar 1D thermal models is then further emphasised insofar as the mechanical performance of the same systems is analysed under the effect of elevated temperatures. At the current stage, for example, the actual role and FE modelling assumptions for common interlayer foils used in laminated glass assemblies - from both a thermal and mechanical point of view - still requires further studies. These aspects are currently under investigation, as an extension of the ongoing research study.

Acknowledgements

References

Aguilar, J.O., Xamán, J., Olazo-Gómez, Y., Hernández-López, I., Becerra, G., & Jaramillo, O.A. (2017). Thermal performance of a room with a double glazing window using glazing available in Mexican market. *Applied Thermal Engineering, 119*: pp.505-515

Aldawoud, A. (2017). Assessing the energy performance of modern glass façade systems. *MATEC Web of Conferences, 120,* paper id: 08001, doi: 10.1051/matecconf/201712008001

Baumgärtner, L., Krasovsky, R.A., Stopper, J., & von Grabe, J. (2017). Evaluation of a solar thermal glass façade with adjustable transparency in cold and hot climates. *Energy Procedia, 122*: pp.211-216

Bedon, C. (2017). Structural glass systems under fire: overview of design issues, experimental research, and developments. *Advances in Civil Engineering, Volume 2017*, Article ID 2120570, 18 pages. Retrieved from https://doi.org/10.1155/2017/2120570

Bedon, C., & Louter, C. (2018). Thermo-mechanical Numerical Modelling of Structural Glass under Fire - Preliminary Considerations and Comparisons. *Proceedings of Challenging Glass Conference, vol. 6*, pp. 513-524, https://doi.org/10.7480/cgc.6.2173

Bedon, C., Honfi, D., & Kozłowski, M. (2018a). Numerical Modelling of Structural Glass Elements under Thermal Exposure. *The 3rd International Electronic Conference on Materials Sciences*. DOI10.3390/ecms2018-05241

Bedon, C., Pascual Agullo, C., Luna-Navarro, A., Overend, M., & Favoino, F. (2018b). Thermo-mechanical Investigation of Novel GFRP-glass Sandwich Façade Components. *Proceedings of Challenging Glass Conference, vol. 6*, pp. 501-512, https://doi.org/10.7480/cgc.6.2172

Bedon, C., Zhang, X., Santos, F., Honfi, D., Kozlowski, M., Arrigoni, M., Figuli, M., & Lange, D. (2018c). Performance of structural glass façades under extreme loads – Design methods, existing research, current issues and trends. *Construction and Building Materials, 163*: pp.921-937

Cardenas, B., Leon, N., Pye, J., & Garcia, H.D. (2016). Design and modeling of high temperature solar thermal energy storage unit based on molten soda lime silica glass. *Solar Energy, 126.* pp.32–43

Cuzzillo, B.R, & Pagni, P.J. (1998). Thermal breakage of double-pane glazing by fire. *Journal of Fire Protection Engineering*, 9(1): 1-11

Debuyser, M., Sjöström, J., Lange, D., Honfi, D., Sonck, D., & Belis, J. (2017). Behaviour of monolithic and laminated glass exposed to radiant heating. *Construction and Building Materials, 130.* pp.212–229

Debuyser, M. (2015). *Exploratory investigation of the behaviour of structural glass in fire.* (Master's Dissertation) Ghent University, Belgium.

Feldmann, M., Kasper, R., Abeln, B., Cruz, P., Belis, J., Beyer, J., Colvin, J., & et al. (2014*). Guidance for European Structural design of glass components – support to the implementation, harmonization and further development of the Eurocodes. In P. Dimova & D. Feldmann (Eds) *Report EUR 26439, Joint Research Centre-Institute for the Protection and Security of the Citizen*. doi: 10.2788/5523.

Fang, Y., Eames, P.C., & Norton, B. (2007). Effect of glass thickness on the thermal performance of evacuated glazing. *Solar Energy, 81(3).* pp.395-404

Favoino, F., Jin, Q., & Overend, M. (2014). Towards an ideal adaptive glazed façade for office buildings. *Energy Procedia, 62.* pp.289-298

Ghosh, A., Norton, B., & Duffy, A. (2016). Measured thermal & daylight performance of an evacuated glazing using an outdoor test cell. *Applied Energy, 177* pp.196-203

Ghoshal, S., & Neogi, S. (2014). Advanced Glazing System - Energy Efficiency Approach for Buildings - A Review. *Energy Procedia, 54.* pp.352-358

Li, D., Li, Z., Zheng, Y., Liu, C., & Lu, L. (2015). Optical performance of single and double glazing units in the wavelength 337-900 nm. *Solar Energy, 122.* pp.1091-1099

Haldimann, M., Luible, A., & Overend, M. (2008). *Structural use of glass.* IABSE, ISBN 978-3-85748-119-2

Hasselaar, B., & Looman, R. (2007). The climate adaptive skin, the integral solution to the conflict between comfort and energy performance. *Proceedings of CIB World Building Congress 2017*, pp. 1115-1125

Miller, C., Thomas, D., Kämpf, J., & Schlueter, A. (2015). Long wave radiation exchange for urban scale modeling within a Co-simulation environment. *Proceedings of CISBAT 2015,* September 9-11, 2015, Lausanne, Switzerland, pp.871-876

Parra, J., Guardo, A., Egusquiza, E., & Alavedra, P. (2015). Thermal performance of ventilated double skin façades with Venetian blinds. *Energies,* 8: 1882-4898, doi: 10.3390/en8064882

prEN thstr:2004. (2004). *Glass in Buildings - thermal stress capitulation method,* CEN, Brussels, Belgium

Simulia. (2018). ABAQUS v. 6.14 computer software and online documentation, Dassault Systems, Providence, RI, USA

Stefanizzi, P., Wilson, A., & Pinney, A. (1990). Internal long-wave radiation exchange in buildings: Comparison of calculation methods: Review of Algorithms. *Building Services Engineering Research and Technology, 11(3)*: pp.81-85

Tong, T.W. (1994). *Thermal Conductivity 22.* Lancaster, PA, USA: Technomic Publishing Company, Ltd.,, ISBN 1-56676-172-7

Tong, S.T., Zhu, L.B., Guo, W., & Ma, F.D. (2002). Numerical simulation on thermal radiation of low emissivity glass surface. *Journal of Building Materials,* 5: pp.60-65

Tofilo, P., & Delichatsios, M. (2010). Thermally induced stresses in glazing systems. *Journal of Fire Protection Engineering*, 20(2): pp.101-116

Wang, T.-P., & Wang, L.-B. (2016). The effects of transparent long-wave radiation through glass on time lag and decrement factor of hollow double glazing. *Energy and Buildings*, 117. pp.33-43

Wang, T.-P., Wang, L.-B., & Li, B.-Q. (2013). A model of the long-wave radiation heat transfer through a glazing. *Energy and Buildings, 59* pp.50-61

Copyright notice